# METHODS ANALYSIS FOR PHASE MEASUREMENT IN WELDED SAMPLE OF SUPERDUPLEX STAINLESS STEEL UNS S32750

*Francisco Magalhães dos Santos Júnior[a,b], Leonardo Oliveira Passos da Silva[a], Luã Fonseca Seixas[a], Tiago Nunes Lima[a], Alexandre Ferraz Dourado[a], Bruno Caetano dos Santos Silva[a], Daniel Marques de Souza[a], Rodrigo Santiago Coelho[a]*

[a] *Forming and Joining, SENAI CIMATEC University Center, Brazil*
[b] magalhaesjun@gmail.com

**Abstract:** This study presents an evaluation of two methods to measure phases in welded samples of super duplex stainless steel UNS S32750. The aim is to identify the most suitable method for characterizing the microstructure of welded joints of this steel. In the color contrast method, it was found that there was no great variation in the results due to the low value of the standard deviation. While for the ASTM E 652 standard point counting method, the percentage values of ferrite found were slightly higher than the previous method. However, these two methods produced low standard deviations and, since the method described by the standard is possible to differentiate deleterious phases, this technique is the most suitable for the microstructure characterization for welded samples of super duplex stainless steel.

**Keywords:** Super duplex stainless steel; Ferrite; Heat-affected zone (HAZ); GTAW; GMAW.

# ANÁLISE DE MÉTODOS PARA CONTAGEM DE FASES EM AMOSTRAS SOLDADAS DO AÇO INOXIDÁVEL UNS S32750

**Resumo:** Neste estudo é apresentada uma avaliação de dois métodos para contagem de fases em amostras soldadas do aço inoxidável super duplex UNS S32750. O objetivo é identificar o método mais adequado para caracterização da microestrutura de juntas soldadas desse aço. No método de contraste de cores, constatou-se que não houve grande variação dos resultados encontrados devido ao baixo valor do desvio padrão. Enquanto que para o método de contagem de pontos da norma ASTM E 652, os valores percentuais de ferrita encontrados foram ligeiramente superiores ao método anterior. No entanto, esses dois métodos produziram baixos desvios padrões e, uma vez que o método descrito pela norma é possível diferenciar fases deletérias, esta técnica é a mais adequada para a caracterização da microestrutura de aço inoxidável super duplex soldados e simulados termicamente.

**Palavras-chave:** Aço inoxidável Super duplex; Ferrita; Zona Termicamente Afetada (ZTA); GTAW; GMAW.

## 1. INTRODUCTION

The Duplex Stainless Steel (DSS) and Super Duplex Steel (SDSS), basically composed of ferrite (δ) and austenite (γ), are materials of great interest for engineering, mainly due to their high resistance to corrosion. Among the stainless steel categories, DSS and SDSS stand out due to their favorable properties combination of ferritic and austenitic stainless steels, combining high mechanical strength, good toughness and resistance to corrosion in aggressive environments [1-3].

The welding parameters of the DSS and SDSS must be strictly controlled, in order to obtain the correct microstructure and keep well/great phase balance between ferrite and austenite. Low thermal input and, consequently, high cooling rate, interfere in the microstructural balance, reducing the volumetric fraction of austenite and, thus, the corrosive resistance. On the other hand, high thermal input and low cooling rate, allow the precipitation of intermetallic phases with consequent weakening of the steel. Due to the high presence of alloying elements in these steels, during the heating and cooling process, the presence of deleterious phases can occur [1, 2, 4, 5].

In the optical microscopy it is possible to show the existence of deleterious phases in the microstructure, even with difficulty in differentiating the shades of the phases. However, there is difficult to differentiate the phases accurately due to the available resolution and the proximity of shades between the sigma (σ) and ferrite (δ) phases, so a certain amount of ferrite, inclusions and other defects can be considered as deleterious phase if not a chemical analysis is performed by Energy Dispersive Spectrometry (EDS), for example [6].

Different techniques can be used to quantify the phases in DSS and SDSS, such as optical microscopy (OM), Scanning Electron Microscopy (SEM), or using a feritscope. Each technique has advantages and disadvantages that need to be considered in order to maximize the quality and speed of results acquisition. The difference between the results for each method was noted by Breda (2015) who conducted a study evaluating the quantification of ferrite by OM (manual and automatic counting), SEM, feritscope and phase diagrams. Research has revealed that the optical microscope is better for quantifying ferrite when compared to other techniques [6, 7].

Using the Electron Backscattered Diffraction technique (EBSD) integrated with SEM, it is possible to obtain maps of phases and other details such as grain boundary, deleterious phases and their quantifications in area fraction. However, this technique requires a long and careful preparation of the samples. The fastest and intermediate precision technique for obtaining the percentage of ferrite in a sample is the analysis made with a feritscope. This technique provides quick information about the amount of the ferritic phase, due to its magnetic property, being a technique using a portable equipment, easy to operate and non-destructive. However, it is not suitable for small areas and doesn't guarantee an exact quantification of ferrite as the processing of the analyzed steel can influence the result, since the size, shape and orientation of the resulting ferrite can significantly modify the magnetic response of this phase [6], [8-10].

Forgas, in 2016, used three techniques to quantify the ferrite content, like: X - Ray Diffraction (XRD), MO with measurements of the phase content by point counting technique according to the ASTM E 562 standard and through the feritscope. They all clearly showed an increase in ferrite content as the temperature increased. The values obtained by quantitative metallography by counting points seemed more assertive, as it is a direct measurement method [10, 11].

No studies were found in the scientific literature comparing the point measurement with the phase contrast technique as methodologies for percentage quantifying of ferrite. In this context, this work aims to compare these two methods to analyze the percentage of phases in welded samples of SDSS UNS S32750, with 10 mm of thickness in order to define which is the most suitable to be applied in phase analysis of project that demand reliability and speed in the response of the results.

## 2. METHODOLOGY

### 2.1. Welding Execution

The 10 mm thick plates were cut into 75 mm by 350 mm joints, using the 1.6 mm thick cutting disc, specifically for stainless steel. A chamfer with a length of 350 mm, 80º chamfer angle, root opening of 3 mm and root face of 1 mm was prepared, as shown in Figure 1. The joint geometry complies with Petrobras N-133 specification. In the regions of cuts and chamfers, mechanical cleaning with grinding and chemical cleaning with acetone was carried out for better finishing during welding, so as not to influence the quality of the welded joints [12].

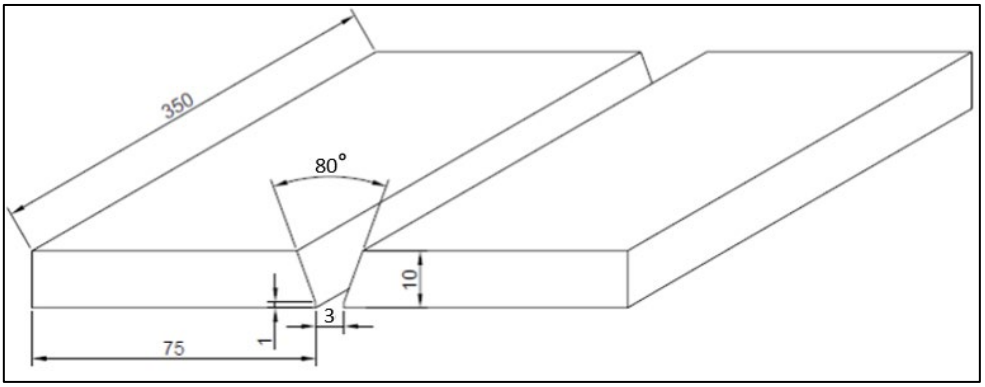


**Figure 1** Geometry of the joint to be welded (units in [mm]).

The welding of the SDSS UNS S32750 was carried out using the infrastructure of SENAI CIMATEC PARK. This welding was carried out in a chamfered joint, parameterized and instrumented to obtain the monitoring of the thermal cycle and process variables such as current, voltage, open arc time, gas flow, welding time and others. The Table 1 lists the equipment used with the respective measured parameters.

**Table 1.** Equipment used with respective monitored parameters.

| MONITORED PARAMETER | EQUIPMENT |
|---|---|
| Open arc time [s]<br>Voltage [V]<br>Current [A]<br>Gas flow [L/s] | SAP suitcase |
| Interpass temperature [°C] | Thermocouples welded by capacitive welding in the region where welding begins |
| Temperature along the plate [°C] | 6-channel temperature monitor with capacitive welded thermocouples |
| Welding time [s] | Professional camera |

For welding, the manual Gas-shielded Tungsten Arc Welding (GTAW) process was used for the first and second passes (root and reinforcement passes) and the mechanized Gas Metal Arc Welding (GMAW) process for the last three passes. In welding with the manual GTAW process, pure argon was used as a shielding gas and to purge the root. In welding through the mechanized GMAW process were used 75% argon gas + 25% $CO_2$ [12].

## 2.2. Macro-structural Characterization

After welding the SDSS UNS S32750, the samples were cut for analysis under a microscope. All cuts perpendicular to the fusion zone were made with a specific cutting disc for stainless steel, 1.6 mm thick, to avoid contamination of the base material.

After the cuts, the sandpaper was used following the granulometries of 180 to 1500, respecting the 90° rotation with each change of sandpaper and lubrication in abundant water. The polishing machine with liquid alumina in suspension was used for metallographic polishing of 1 μm and 0.3 μm, in a rotation of 300 rpm. After sanded and polished, the samples were subjected to 3V electrolytic etching for about 7 seconds using a 40% potassium hydroxide solution as a reagent (adapted Murakami reagent) [13]. Electrolytic attacks were carried out by connecting each sample submerged in the 40% KOH solution to the cathode and a titanium bar to the anode of the power supply [5]. The images for analysis of the passes were obtained by a Zeiss optical microscope and AxioCam ERC 5s model.

## 2.3. Phase Measurement

The phase measurement analyzes were performed using two methods. The color contrast method used the software Photoshop and ImageJ. The images obtained by the microscope were treated in Photoshop to adjust contrast and brightness, as well as adjusting each grain in the micrograph so that it would be suitable for applying the phase measurement in ImageJ. In the latter, the counting is performed from the threshold adjustment (converts gray or colored images into high contrast black and white images) and then the percentage of black (ferrite) and white (austenite) pixels is counted by the software itself [14].

The second method used for phase counting was following the ASTM E 562 standard, also in line with the changes determined by Petrobras' standard I-ET-3010.90-1200-955-PPC-002. The photographs must be covered with a grid of at least 100 points and the percentage of ferrite must be calculated from the number of points under the ferritic phase and the total number of points used. To obtain a result with greater precision of covering the phases and in a larger area, a 14x14 grid was used, that is, 196 points [11, 15].

$$\%Phase = \frac{Points\ under\ the\ ferritic\ phase}{Total\ grid\ points} \times 100 \quad (1)$$

ASTM E 562 indicates that any image scale can be used, as long as it is possible to identify the different phases. For both methods, images of the upper, central and lower sections of the base metal region and the HAZ were analyzed, totaling three images from each region and two grids per image [11].

## 3. RESULTS AND DISCUSSION

### 3.1. Welding Parameters

By monitoring the welding parameters, it was possible to obtain the heat input of each bead and pass. Table 2 shows the parameters used and the heat input calculated for welding. The values of current, voltage, travel speed and heat input of the root pass, first pass, were disregarded due to inconsistencies in the capture of the monitored data.

**Table 2.** Parameters used in welding SDSS UNS S32750.

| PASS | HEAT INPUT [kJ/mm] | CURRENT [A] | VOLTAGE [V] | TRAVEL SPEED [mm/min] |
|---|---|---|---|---|
| **1** | - | - | - | - |
| **2** | 0,66 | 146,0 | 12,5 | 166,1 |
| **3** | 0,60 | 114,5 | 32,0 | 365,6 |
| **4** | 0,59 | 112,0 | 31,9 | 365,2 |
| **5** | 0,61 | 103,4 | 31,9 | 324,9 |

### 3.2. Phase Analysis

The same images treated by Photoshop software were used for both methods to facilitate comparison between them. The result of the color contrast methodology is presented in the Figure 1 and it can be seen that there was no great variation in the ferrite content between the three sections analyzed, (upper, central and lower of the fusion zone) due to the low value of the standard deviation (Base Metal: ± 2,35 and HAZ: ± 1,66). It is also verified that the value of the average percentage of ferrite from HAZ, of the three sections, is very close to the value of the base metal and within the specifications of Petrobras, between 40% and 60% of ferrite [1, 4, 11, 14, 15].

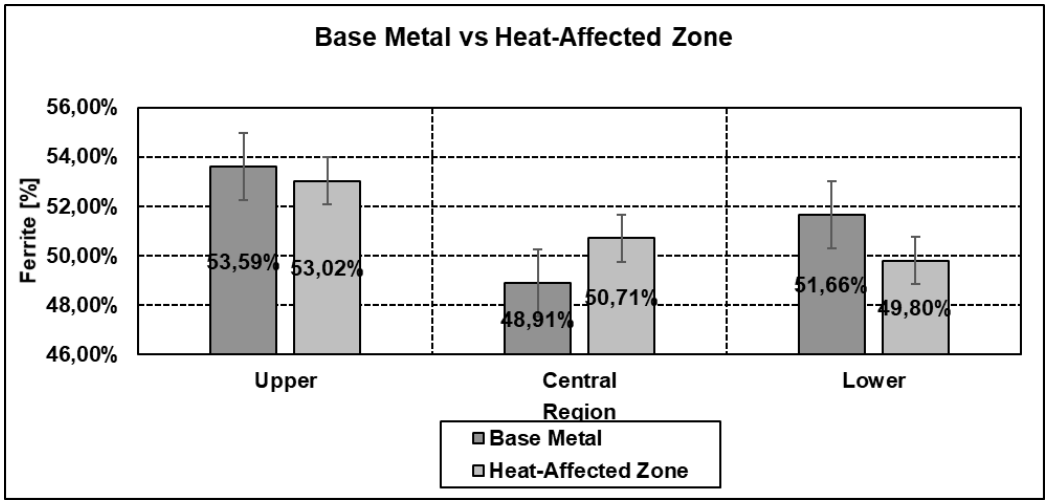


**Figure 1.** Results of phase measurement by the color contrast method

The result, using the method described in the ASTM E 562 standard, for counting points, is shown in Table 3. The ferrite values found by this method were slightly higher than by the previous method, but remained within the range recommended by Petrobras standards and close ferrite values between the base metal

and the HAZ. The color contrast method was the one with the lowest standard deviation, although the difference between the deviations was not significant. The two methods showed similar results, revealing that the techniques converge to the ferrite measurement present in the material [11, 14].

**Table 3.** Results of phase measurement using the ASTM E 562 standard method.

| Region | 10 mm (ASTM E 562) | | | |
|---|---|---|---|---|
| | Base Metal | | Heat-Affected Zone | |
| | Points | % Ferrite | Points | % Ferrite |
| **Upper (1)** | 106 | 54,08% | 117 | 59,69% |
| **Upper (2)** | 110 | 56,12% | 105 | 53,57% |
| **Central (1)** | 98 | 50,00% | 114 | 58,16% |
| **Central (2)** | 96 | 48,98% | 103 | 52,55% |
| **Lower (1)** | 108 | 55,10% | 104 | 53,06% |
| **Lower (2)** | 109 | 55,61% | 110 | 56,12% |
| **Medium (stand. dev.)** | 53,32% ± 3,06 | | 55,53% ± 2,95 | |

The original metallographic and treated images are presented in the Figure 2 and Figure 3 and served to quantify the ferrite phase of the base metal and HAZ, respectively.

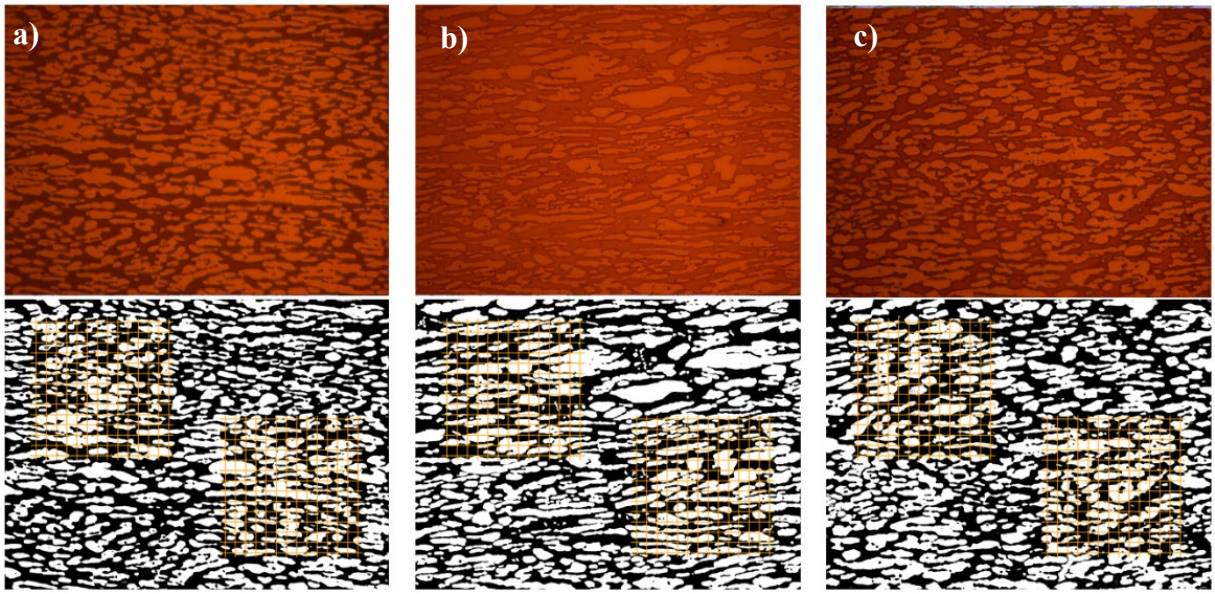


**Figure 2.** Micrographs before and after image treatment for counting the base metal phases. Upper, central and lower regions in (a), (b) and (c) respectively.

ISSN: 2357-7592

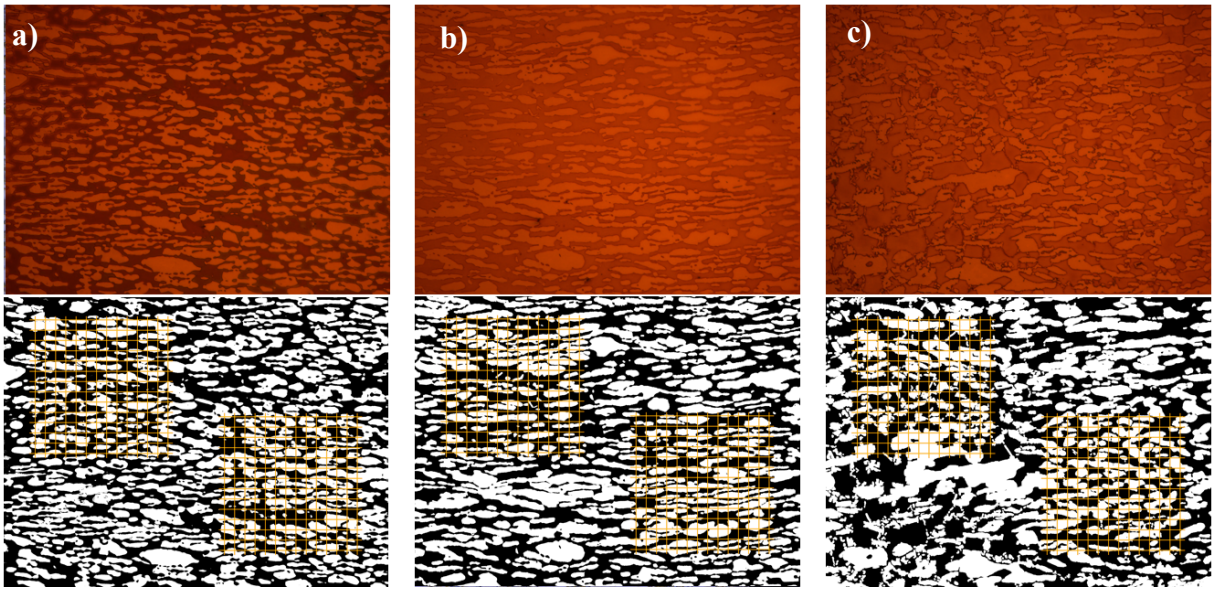


**Figure 3.** Micrographs before and after image treatment for phase counting of the thermally affected zone. Upper, central and lower regions in (a), (b) and (c) respectively.

Deleterious phases are prone to form during the welding process, such as carbide, sigma phase, chi phase, chromium nitride and secondary austenite. These precipitations can cause a deterioration of the mechanical and corrosion properties in SDSS welds [16]. These unwanted phases were not objective in this work, which focused only on the identification of ferritic phases.

## 4. CONCLUSION

Despite having the slowest execution due to the need to insert grids in the micrographs, the ASTM E 562 method is standardized and has managed to produce good results and with low standard deviations, demonstrating that it is the most appropriate phase counting technique to be used during stages of the project that demand fast and reliable results. It is also important to note that the color contrast method, by analyzing only black and white pixels, is not able to differentiate harmful phases if there is one, making the ASTM E 562 standard more suitable for this case.

## 5. REFERENCES

1 Z. Zhang, H. Zhao, H. Zhang, J. Hu, and J. Jin, "**Microstructure evolution and pitting corrosion behavior of UNS S32750 super duplex stainless steel welds after short-time heat treatment**," *Eval. Program Plann.*, vol. 121, pp. 22–31, 2017, doi: 10.1016/j.corsci.2017.02.006.

2 G. Chail and P. Kangas, "**Super and hyper duplex stainless steels: Structures, properties and applications**," *Procedia Struct. Integr.*, vol. 2, pp. 1755–1762, 2016, doi: 10.1016/j.prostr.2016.06.221.

3 L. O. P. da Silva, A. C. Nascimento, F. M. dos Santos Júnior, T. N. Lima, B. C. dos S. Silva, and R. S. Coelho, "**Simulação Numérica E Física Na Soldagem Dos Aços Inoxidáveis Duplex: Uma Revisão Sistemática.**," pp. 373–380,

2019, doi: 10.5151/siintec2019-47.

[4] M. Schütze, **Corrosion Books: Handbook of Corrosion Engineering**. By Pierre R. Roberge - Materials and Corrosion 4/2002, vol. 53, no. 4. 2002.

[5] R. O. Dos Santos, M. R. S. Almeida, L. L. N. Guarieiro, and R. S. Coelho, "**Analysis of the GTAW process influence on UNS S32760 superduplex steel microstructure and corrosion resistance**," *Rev. Virtual Quim.*, vol. 8, no. 4, pp. 1040–1053, 2016, doi: 10.21577/1984-6835.20160074.

[6] F. Ribeiro, "**Aplicação De Diferentes Técnicas De Microscopia Para A Quantificação De Fases Deleté Rias Presentes No Aço Inoxidável Superduplex Uns S32750**," Fortaleza, 2017.

[7] M. Breda, J. Basoni, F. Toldo, C. Bastianello, S. A. Ontiveros Vidal, and I. Calliari, "**Comparative analysis on phase quantification methods in duplex stainless steels weldments**," *Metall. Ital.*, vol. 107, no. 4, pp. 3–7, 2015.

[8] G. C. de Souza *et al.*, "**Avaliação da Proporção de Fases em Juntas Soldadas de Tubulações de Aço Inoxidável Duplex Mediante Aplicação de Ensaios Não Destrutivos**," *Soldag. e Insp.*, vol. 18, no. 2, pp. 158–168, 2013, doi: 10.1590/S0104-92242013000200009.

[9] C. G. Camerini *et al.*, "**Avaliação Do Ferritoscópio Para Quantificação De Ferrita Delta Em Aços Inoxidáveis Superduplex**," vol. 72, pp. 2491–2501, 2017, doi: 10.5151/1516-392x-30710.

[10] A. Forgas Júnior, J. Otubo, and R. Magnabosco, "**Ferrite quantification methodologies for duplex stainless steel**," *J. Aerosp. Technol. Manag.*, vol. 8, no. 3, pp. 357–362, 2016, doi: 10.5028/jatm.v8i3.653.

[11] Astm, "**Standard Test Method for Determining Volume Fraction by Systematic Manual Point Count E 562**," *Practice*, no. C, pp. 1–7, 2011, doi: 10.1520/E0562-11.2.

[12] A. Normas, "**N-133 Soldagem**," 2017.

[13] I. N. Bastos and R. P. Nogueira, "**Electrochemical noise characterization of heat-treated superduplex stainless steel**," *Mater. Chem. Phys.*, vol. 112, no. 2, pp. 645–650, 2008, doi: 10.1016/j.matchemphys.2008.06.034.

[14] D. Arun, K. D. Ramkumar, and R. Vimala, "**Multi-pass arc welding techniques of 12 mm thick super-duplex stainless steel**," *J. Mater. Process. Tech.*, vol. 271, no. March, pp. 126–143, 2019, doi: 10.1016/j.jmatprotec.2019.03.031.

[15] Petrobras, "**Technical Specification** I-ET-3010.90-1200-955-PPC-002," 2000.

[16] Z. Zhang, Z. Wang, Y. Jiang, H. Tan, D. Han, and Y. Guo, "**Effect of post-weld heat treatment on microstructure evolution and pitting corrosion behavior of UNS S31803 duplex stainless steel welds,**" *Corros. Sci.*, vol. 62, pp. 42–50, 2012, doi: 10.1016/j.corsci.2012.04.047.